


## Material-based analysis of spin-orbital Mott insulators

Ryuta Iwazaki<sup>✉</sup>, Hiroshi Shinaoka<sup>✉</sup>, and Shintaro Hoshino

Department of Physics, Saitama University, Shimo-Okubo, Saitama 338-8570, Japan

 (Received 24 January 2023; revised 22 November 2023; accepted 27 November 2023; published 12 December 2023)

We present a framework for analyzing Mott insulators using a material-based tight-binding model. We start with a realistic multiorbital Hubbard model and derive an effective model for the localized electrons through the second-order perturbation theory with respect to intersite hopping. This effective model, known as the Kugel-Khomskii model, is described by  $SU(N)$  generators, where  $N$  is the number of localized states. We solve this model by the mean-field theory that takes local correlations into account and reveal spin-orbital ordered states. To include spatial correlations, we apply the classical Monte Carlo based on the path-integral approach with  $SU(N)$  coherent states, and also derive the equation of motion for spin-orbital degrees of freedom. Our approach enables quantitative analysis of Mott insulator materials with a small intersite quantum correlation. The  $5d$ -pyrochlore oxide is used here as a demonstration.

DOI: [10.1103/PhysRevB.108.L241108](https://doi.org/10.1103/PhysRevB.108.L241108)

**Introduction.** Multiorbital systems with strongly correlated electrons have been attracting attention due to their diverse physical phenomena, such as electronic ordering and multiferroic behavior. It is crucial to uncover their material-specific physical properties in order to make a serious comparison with experimental results. In materials with weakly correlated electrons, density functional theory (DFT)-based calculations have been successful in describing their electronic properties. On the other hand, in the strongly correlated regime, it is useful to construct a tight-binding model using localized Wannier functions and subsequently employ a multiorbital Hubbard model with local Coulomb repulsive interactions as a fundamental model. Unfortunately, it is extremely difficult to perform the calculations in a realistic setting due to the immense numerical cost. A theoretical framework that is applicable to realistic strongly correlated electron systems is highly desired, which will enable material prediction through, for example, high-throughput screening [1].

In the present work, we focus on the Mott insulators where the electrons are localized with a strong local Coulomb interaction. Even in this case, the spin-orbital degrees of freedom generate a number of interesting phenomena such as magnetic orderings, multiferroic behaviors, and spin liquids [2–10]. The low-energy effective model with localized electrons is known as the Kugel-Khomskii model, in which both the spin and orbital degrees of freedom are involved [11–27]. The realistic localized models have been discussed for the spin model [28–39] and  $e_g/t_{2g}$ -multiorbital systems [40–46]. The DFT+DMFT approaches have also been employed for the analysis [28,39–42,47–49]. In order to study *arbitrary* Mott insulator materials, however, a more general framework is needed that can be applied at a reasonable computational cost to general multiorbital systems with spin-orbit interactions and any number  $N$  of localized states per atom.

In this Letter, we propose a general framework to perform calculations for the spin-orbital Mott insulators, which is not restricted to specific systems. We develop a realistic spin-orbital model based on the tight-binding model derived

from first-principles calculations and the local Coulomb interaction with Slater-Condon parameters. The model contains  $N^2 - 1$  spin-orbital degrees of freedom and is described by  $SU(N)$  generators. When analyzing the model, while a fully quantum analysis is not feasible because of the huge computational cost, we use the classical Monte Carlo with the  $SU(N)$  coherent state [50–52], in addition to the standard mean-field theory. The  $SU(N)$  coherent state has been used for the spin systems [53–62], and here we apply it to the realistic spin-orbital model. While the quantum-mechanical intersite correlations at very low temperatures are not incorporated in our theory, our method captures the characteristic physics at finite temperatures in a realistic setup for any Mott insulators with a reasonable numerical cost.

We will take the pyrochlore oxide  $Cd_2T_2O_7$  as an example. This is suitable as a prototype material for the demonstration of our framework due to its complicated electronic structure: the four transition-metal  $T$  atoms in unit cell (specified as sublattice indices A, B, C, D), large spin-orbit interaction, and  $t_{2g}$  three orbitals of  $5d$  electrons with trigonal symmetry at  $T$  atom site [63,64] (see Fig. 1). In addition, their noncollinear magnetic structures are well studied both theoretically and experimentally [65,66]. Hence the applicability to this prototypical material  $Cd_2T_2O_7$  demonstrates the versatility of our method.

**Realistic spin-orbital model.** The realistic effective model for the localized electrons is constructed based on the multiorbital Hubbard model derived from first-principles calculations. Let us begin with the Hamiltonian  $\mathcal{H} = \mathcal{H}_{\text{loc}} + \mathcal{H}_t$ , where

$$\mathcal{H}_t = \sum_{\langle ij \rangle} \sum_{ab} t_{ij}^{ab} c_{ia}^\dagger c_{jb} + \text{H.c.} \quad (1)$$

describes the intersite hopping term. The operator  $c_{ia}$  annihilates the electron at the atom site  $i$  with the spin ( $\sigma$ )-orbital ( $\gamma$ ) index  $a = (\gamma, \sigma)$ . The symbol  $\langle ij \rangle$  indicates the summation with respect to the pairs of atomic sites, and includes the terms other than those of the nearest-neighbor sites. The

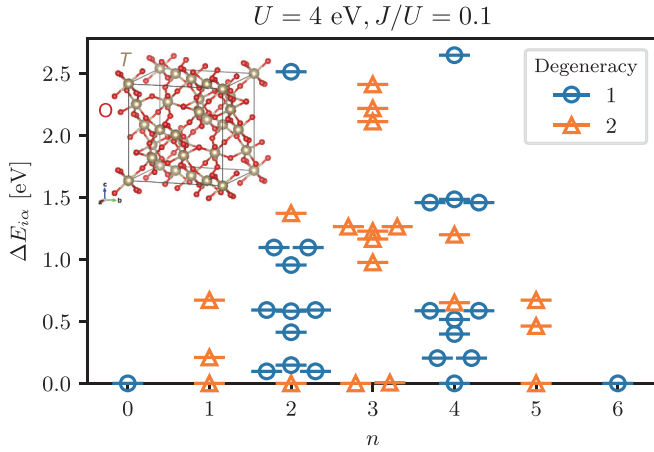


FIG. 1. Single-site eigenenergy levels for  $\text{Cd}_2\text{T}_2\text{O}_7$ , which corresponds to  $\mathcal{H}_t = 0$ . We choose  $U = 4$  eV and  $J/U = 0.1$ , which is comparable to the previous study [71]. The vertical axis shows the energy measured from the lowest energy at each  $n$ . The inset is the crystal structure of  $\text{Cd}_2\text{T}_2\text{O}_7$ , where only  $T$  and  $O$  atoms are shown for clarity [72].

local part  $\mathcal{H}_{\text{loc}}$  is further divided into three components as  $\mathcal{H}_{\text{loc}} = \mathcal{H}_U + \mathcal{H}_{\text{SOC}} + \mathcal{H}_{\text{CEF}}$ , which are the Coulomb interaction, the spin-orbit coupling and the local crystalline electric field, respectively. The Coulomb interaction is written as

$$\mathcal{H}_U = \sum_{i\gamma_1\gamma_2\gamma_3\gamma_4\sigma\sigma'} U_{\gamma_1\gamma_2\gamma_3\gamma_4} c_{i\gamma_1\sigma}^\dagger c_{i\gamma_2\sigma'}^\dagger c_{i\gamma_4\sigma} c_{i\gamma_3\sigma}, \quad (2)$$

which is parameterized by the Slater-Condon parameters as typically used in LDA+ $U$  or LDA+DMFT framework [67]. Specifically for the three orbital case as in  $t_{2g}$  orbital, the standard Slater-Kanamori form is employed:  $U_{\gamma\gamma\gamma\gamma} = U/2$ ,  $U_{\gamma\gamma'\gamma\gamma'} = U'/2$ ,  $U_{\gamma\gamma'\gamma'\gamma} = U_{\gamma\gamma\gamma'\gamma'} = J/2$  for  $\gamma \neq \gamma'$  ( $U' = U - 2J$ ) and the other terms are zero.

In the following, we take the tight-binding model of  $T = \text{Os}$  derived from an electronic-structure calculation [68]. Since the band structure [see Fig. 2(a)] is similar to that of other materials with different fillings such as  $T = \text{Re}$  [69,70], we use the data of the  $T = \text{Os}$  case also for other electron fillings.

We analyze the multi-orbital Hubbard model in the strong coupling limit ( $U \rightarrow \infty$ ), where the electrons are localized. First of all, we derive the eigenenergies and eigenfunctions in the atomic model with only  $\mathcal{H}_{\text{loc}}$ , which is necessary for specifying the model Hilbert space at low energies, i.e., the number  $N$  of the localized states. Figure 1 shows the single-site eigenenergy diagram of  $\mathcal{H}_{\text{loc}}$  for each number  $n$  of electrons per  $T$  atom. When we focus on the odd number of the filling  $n$ , there are only doubly degenerate states corresponding to the Kramers doublet.

In this paper, we choose  $n = 1$  for a demonstration of our scheme, which allows us to choose the size of the model space as  $N = 2, 4, 6$  based on Fig. 1. We call them SU(2), SU(4), and SU(6) models, respectively. The SU( $N$ ) model contains  $N^2 - 1$  operators for each atom. The procedure for the simplest  $N = 2$  case is summarized in the Supplemental Material (SM) [68]. Although the dimension of the model Hilbert space may be dependent on the lattice site, we here take the same  $N$  for all the sites.

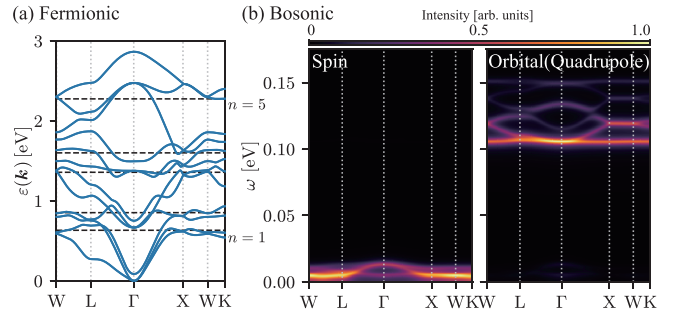


FIG. 2. (a) Electronic energy bands for  $\text{Cd}_2\text{T}_2\text{O}_7$ . The vertical axis is measured from the bottom of the bands. The horizontal dashed lines express the chemical potential for each  $n$ . (b) Bosonic energy spectra  $\text{Im}\chi(\mathbf{q}, \omega)/\omega$  for the SU(6) model at  $T = 10^{-3}$  eV. The left panel shows the dispersion for the spin, while the orbital excitation spectra is shown in the right panel.

In order to understand the validity of the low-energy model, it is convenient to recognize the three energy scales: the intersite interaction  $I \sim zt^2/U$  with a coordination number  $z$ , the energy difference between the different electron numbers  $U$ , and the single-site energy splitting  $\Delta (\ll U)$  for a fixed number of electrons. The localized electron model is justified for  $U \gg I$ , which is the necessary condition for the present framework. If  $\Delta \gg I$  is satisfied, the SU(2) model is justified for  $n = 1$ . Otherwise, the SU(6) model needs to be considered for a quantitative analysis.

Let us now evaluate whether the above relation is satisfied. In our model, the maximum absolute value of the nearest-neighbor intersite hopping is estimated to be  $t \sim 0.2$  eV. Substituting this value into the above expression, we obtain the intersite coupling constant as  $I \sim 0.06$  eV with  $z = 6$  for the number of nearest-neighbor sites of the pyrochlore lattice. According to Fig. 1, the energy gap between the ground state and the first excited state for  $n = 1$  is  $\Delta \sim 0.2$  eV. Consequently, the assumption  $\Delta \gg I$  is not fully justified, and this may lead to a quantitative difference between the SU(2) and the SU(4) or the SU(6) model. A comparison of the number of the model Hilbert space will be addressed later.

Once the model space is specified, we treat the intersite Hamiltonian  $\mathcal{H}_t$  as a perturbation to obtain the effective Hamiltonian, which gives correct eigenenergies within the restricted Hilbert space [73–77]. While there are several choices of the form of the effective Hamiltonian, the Hermitian Hamiltonian (des Cloizeaux type) is easier to be handled [75,76]. We focus on the two atoms, which are connected by the hopping matrix  $\mathcal{H}_t$ , and expand this two-site Hamiltonian up to the second order of  $\mathcal{H}_t$  [68]. Thereby we obtain the matrix element of the effective Hamiltonian whose size is  $N^2 \times N^2$ . We can rewrite the obtained effective Hamiltonian by complete local operators  $\mathcal{O}_i$  at the site  $i$ . We employ the numerical calculation with matrix multiplications for this procedure [78]. Collecting all the combinations of the two-site Hamiltonians, we obtain the following realistic spin-orbital model:

$$\mathcal{H}_{\text{eff}}[\mathcal{O}] = \sum_{(ij)} \sum_{\xi\xi'} I_{ij}^{\xi\xi'} \mathcal{O}_i^\xi \mathcal{O}_j^{\xi'} - \sum_i \sum_{\xi} H_i^\xi \mathcal{O}_i^\xi, \quad (3)$$

where both the zeroth- and second-order contributions are involved in this effective Hamiltonian. The second term describes the SOC and CEF effects in the original electron systems. We have defined the local operators  $\mathcal{O}_i^\xi = \sum_{\alpha\beta} O_{\alpha\beta}^\xi |\alpha\rangle_i \langle\beta|$  ( $\alpha = 1, \dots, N, \xi = 0, \dots, N^2 - 1$ ), where  $|\alpha\rangle_i$  is a state vector in the model Hilbert space at site  $i$ . We use the matrices  $O_{\alpha\beta}^\xi$  with completeness and orthonormality [e.g., for single orbital model, we take the SU(2) generators, which are the Pauli matrices] [68]. We emphasize that this Hamiltonian is derived from the first-principles calculation data, where the tunable parameters are only the local Coulomb interaction parameters  $U$  and  $J$ . In the actual calculation, the data of  $I_{ij}^{\xi\xi'}$  is outputted with the data structure similar to the original input of  $t_{ij}^{ab}$ .

Since it is in general difficult to interpret the physical meaning of the local operators  $\mathcal{O}_i^\xi$ , it is desirable to transform them into physical quantities defined in terms of the original electronic system. Let us consider the local physical quantity  $\mathcal{A}_i$ . This can be a spin or orbital operator if we choose the form of  $\mathcal{A}_i = \frac{1}{2} \sum_{ab} A_{ab} c_{ia}^\dagger c_{ib}$  where the matrix  $A$  is composed of a direct product of the matrices in spin and orbital spaces. By using the projection operator onto the model Hilbert space,  $\mathcal{P} = \prod_i \sum_\alpha |\alpha\rangle_i \langle\alpha|$ , we obtain

$$\mathcal{P} \mathcal{A}_i \mathcal{P} = \sum_\xi \mathcal{O}_i^\xi \sum_{\alpha\beta} {}_i \langle\alpha|\mathcal{A}_i|\beta\rangle_i \mathcal{O}_{\beta\alpha}^\xi. \quad (4)$$

We can get the matrix element  ${}_i \langle\alpha|\mathcal{A}_i|\beta\rangle_i$  by analyzing  $\mathcal{H}_{\text{loc}}$ . Thus, once the expectation value of  $\mathcal{O}_i$  is obtained by solving the model in Eq. (3), any local physical quantities can be evaluated through this formula. For example, we can calculate the magnetic moment by a linear combination of the spin ( $\mathcal{A}_i = S_i$ ) and the magnetic orbital moment ( $\mathcal{A}_i = L_i$ ) [68]. In addition, it is notable that one can choose the local many-body physical quantities, such as double occupancy expressed as  $\mathcal{A}_i = \sum_\gamma c_{i\gamma\uparrow}^\dagger c_{i\gamma\downarrow}^\dagger c_{i\gamma\downarrow} c_{i\gamma\uparrow}$ , which are not usually considered in conventional spin-orbital models.

The correlation functions are also useful quantities. When we consider the linear response against a small fictitious field conjugate to  $\mathcal{O}_i^\xi$ , the dynamical susceptibilities are given by

$$\chi_{ij}^{\xi\xi'}(iv) = \int_0^{1/T} d\tau [\langle \mathcal{O}_i^\xi(\tau) \mathcal{O}_j^{\xi'} \rangle - \langle \mathcal{O}_i^\xi \rangle \langle \mathcal{O}_j^{\xi'} \rangle] e^{iv\tau}, \quad (5)$$

where  $\mathcal{O}_i^\xi(\tau) = e^{\tau\mathcal{H}} \mathcal{O}_i^\xi e^{-\tau\mathcal{H}}$ .  $\tau$  is the imaginary time in the Heisenberg picture, and  $\nu = 2\pi mT$  ( $m \in \mathbb{Z}$ ) is a bosonic Matsubara frequency. We have taken  $k_B = 1$ . Using Eq. (4), the susceptibility can be transformed into the physical susceptibilities defined in terms of the original electron operators. The information of any spin-orbital excitation is encoded in Eq. (5). For example, we can obtain the dispersion of the orbital, which is a quasiparticle describing the excitation of the orbital [13,17,19].

*Mean-field theory.* Since the obtained localized model contains quantum effects, it is still very hard to be solved. In the following, we introduce several approximate methods to solve the realistic spin-orbital model given in Eq. (3). The most fundamental approximation is the mean-field theory. Defining the effective field  $\tilde{H}_i^\xi = H_i^\xi - \sum_{j \neq i, \xi'} I_{ij}^{\xi\xi'} M_j^{\xi'}$ , the mean-field

Hamiltonian is written as

$$\mathcal{H}_{\text{MF}} = - \sum_i \sum_\xi \tilde{H}_i^\xi \mathcal{O}_i^\xi - \sum_{(ij)} \sum_{\xi\xi'} I_{ij}^{\xi\xi'} M_i^\xi M_j^{\xi'}. \quad (6)$$

We have defined  $M_i^\xi = \text{Tr}(\mathcal{O}_i^\xi e^{-\mathcal{H}_{\text{MF}}/T}) / \text{Tr} e^{-\mathcal{H}_{\text{MF}}/T}$ . In the mean-field calculation, we focused on  $\mathbf{q} = \mathbf{0}$  type orderings. This is justified by the classical Monte Carlo calculation as discussed later [see Fig. 4(b)].

We also evaluate the dynamical susceptibilities with the random phase approximation as

$$\hat{\chi}(\mathbf{q}, \omega) = \hat{\chi}_0(\omega) [\hat{1} + \hat{I}(\mathbf{q}) \hat{\chi}_0(\omega)]^{-1}, \quad (7)$$

where the hat ( $\hat{\cdot}$ ) symbol represents the matrix with respect to the index  $\xi$ , and  $\hat{1}$  is the identity matrix. We have defined the local susceptibility by  $\hat{\chi}_0(\omega) = \hat{\chi}_{ii}(\omega + i0^+)$ , which is evaluated by the local mean-field Hamiltonian.

First of all, we show in Fig. 2(b) the spin-orbital excitation spectra of the realistic spin-orbital model, which is contrasted against the fermionic excitation of the original tight-binding electrons in Fig. 2(a). We take the SU(6) model at  $n = 1$  and  $T = 10^{-3}$  eV. The left panel of Fig. 2(b) is the spin-orbital entangled spectra probed by spin, which corresponds to the dispersion of the magnon. More specifically, we have considered the dynamical correlation function of the spin operator in Eq. (4). The gapped excitation reflects the presence of the spin-orbit coupling. The right panel is the spectra for the nonmagnetic orbital (quadrupole) moment (see Ref. [68] for the definition of the orbital moment). This orbital excitation is unique to the SU(6) model, although the magnon dispersion is captured already in the SU(2) model.

We show the temperature dependence of the order parameters at A sublattice in Fig. 3(a) for the SU(6) model. The symbols  $S$ ,  $L$ ,  $Q$ ,  $G$ , and  $T$  are the spin, magnetic orbital, electric orbital (quadrupole), electric dipole, and magnetic octupole moments, respectively [68].  $Q^{xy}$ ,  $Q^{yz}$ , and  $Q^{zx}$  moments gradually increase with decreasing temperature. These three components take the same value, reflecting the three-fold rotational symmetry along the local [1,1,1] direction. At low temperatures with  $T \lesssim 10^{-2}$  eV, the magnetic ordering occurs, whose order parameters are described by  $S$ ,  $L$ , and  $T$ . We also show the  $\mathbf{q} = \mathbf{0}$  component of the diagonal susceptibilities at A sublattice in Fig. 3(b), where the magnetic susceptibilities ( $S$ ,  $L$ ,  $T$ ) diverge. The magnetic structures at  $T = 10^{-3}$  eV are shown at Fig. 3(c), which displays the all-in-all-out (AIAO) structure and the antiparallel alignment of  $S$  and  $L$  moment. The AIAO-type magnetic ordering in 5d-pyrochlore oxides has been suggested both theoretically and experimentally [65,66,71,79–81].

The temperature dependence of the thermodynamic quantities per site are shown in Fig. 3(d), with which we compare the results of the SU(2,4,6) models. All of the models have an anomaly in the specific heat (bottom panel) around  $T_c \simeq 10^{-2}$  eV, which signals a second-order phase transition. The SU(6) model has a smaller magnetic transition temperature compared to the SU(2,4) cases. The single site entropy (top panel) has a  $\ln 2$  plateau for the SU(4) and the SU(6) model just above  $T_c$ , and it deviates from  $\ln 2$  reflecting the additional degrees of freedom at higher  $T$ . The specific heat above  $T_c$

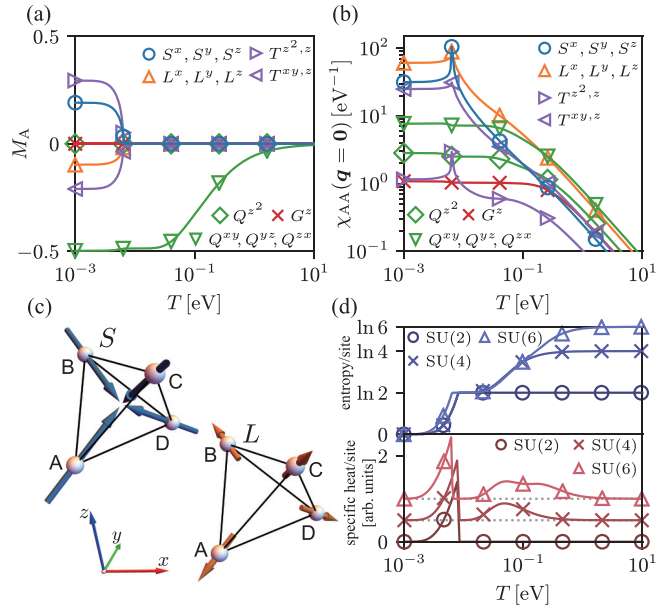


FIG. 3. Temperature dependence of (a) the order parameters and (b) the  $\mathbf{q} = \mathbf{0}$  component of the static diagonal susceptibilities at A site for the SU(6) model obtained by the mean-field analysis. The blue, orange, green, red, and purple lines show the spin, magnetic orbital, electric orbital, electric dipole, and magnetic octupole, respectively. (c) Sketches for the spin ( $S$ ) and the magnetic orbital moment ( $L$ ) of the SU(6) model at  $T = 10^{-3}$  eV. (d) Temperature dependence of the entropy (top panel) and the specific heat (bottom panel) with the circles, crosses and triangles for the SU(2), SU(4), and SU(6) models, respectively. For clarity, the specific heat is vertically shifted for the SU(4,6) models.

shows Schottky peaks originating from the local energy-level splitting.

*Classical model.* We can also solve the model by applying the classical approximation to Eq. (3). In this method, we can examine the effect of the nonlocal correlation. We employ the path-integral formalism using a coherent state [52,55], with which we derive both the classical partition function and equations of motion. The coherent state is defined for each site  $i$  by

$$|\Omega_i\rangle = \sum_{\alpha=1}^N c_{\alpha}(\Omega_i)|\alpha\rangle_i, \quad (8)$$

where  $|\alpha\rangle_i$  is a quantum state basis.  $\Omega_i$  is a set of local continuous variables:  $\Omega_i = \{\xi_{1i}, \dots, \xi_{N-1,i}, \varphi_{1i}, \dots, \varphi_{N-1,i}\}$ , each of which is written as  $\Omega_{pi}$  [ $p = 1, \dots, 2(N-1)$ ] [68]. Here  $\xi_{1i}, \dots \in [0, \pi/2]$  and  $\varphi_{1i}, \dots \in [0, 2\pi)$ , respectively, correspond to the generalized versions of polar angle and azimuthal angle of the spin in the SU(2) model.

The partition function is written as  $Z = \int \mathcal{D}\Omega e^{-\mathcal{S}}$ , where the action is [53]

$$\mathcal{S} = \int d\tau (\langle \Omega | \partial_{\tau} | \Omega \rangle + \langle \Omega | \mathcal{H}_{\text{eff}} | \Omega \rangle). \quad (9)$$

We have defined  $|\Omega\rangle = \prod_i |\Omega_i\rangle$  at an imaginary time  $\tau$ . The quantum-mechanical operator  $\mathcal{O}_i$  is now replaced by the classical variable:  $\mathcal{O}^{\xi}(\Omega_i) = \langle \Omega | \mathcal{O}_i^{\xi} | \Omega \rangle$ . Based on these

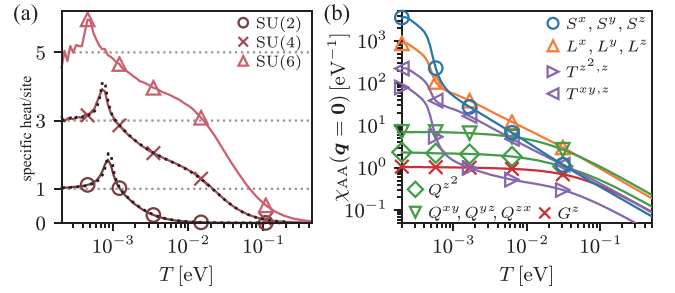


FIG. 4. (a) Temperature dependence of the specific heat per site for the SU(2,4,6) models indicated by circles, crosses and triangles, respectively, which are obtained by the classical Monte Carlo method. The black dotted lines for the SU(2,4) models are the results with  $N_{\text{site}} = 256 (= 4 \times 4^3)$ . (b) Temperature dependence of the  $\mathbf{q} = \mathbf{0}$  component of the diagonal susceptibilities at A site for the SU(6) model.

expressions, the classical model can be rigorously derived by using the coherent state path integral method that omits the Berry phase term, as in the spin model [82]. We can also show that the classical free energy is always larger than the quantum one [83], and it is ensured that the lowest-free-energy state in the classical model is energetically closest to the genuine quantum state.

The model can be numerically simulated by using the classical Monte Carlo method. We use the local Metropolis update and the replica exchange method, which allows us to simulate the systems with various temperatures efficiently [84]. In addition, we also apply the overrelaxation update [85] for the more efficient simulation. The overrelaxation update in the present case consists of microcanonical moves that does not alter the energy. For the SU(2) case, the local spin vector is rotated around the local effective field by the angle  $\pi$  [86,87]. However, this cannot be directly extended to SU( $N$ ) case, and the consideration based on the coherent state is needed.

To perform the overrelaxation update for the SU( $N$ ) case, let us focus on the one lattice site  $i$ , and then its effective local Hamiltonian is written as  $\mathcal{H}_{\text{loc},i} = -\sum_{\xi} \tilde{H}_i^{\xi} \mathcal{O}^{\xi}(\Omega_i)$  where the effect of the surrounding sites is included in  $\tilde{H}_i^{\xi} = H_i^{\xi} - \sum_{j \neq i, \xi'} I_{ij}^{\xi \xi'} \mathcal{O}(\Omega_j)$ , which is not dependent on  $\Omega_i$ . We can cast it into the coherent state representation as

$$\mathcal{H}_{\text{loc},i} = \sum_{\alpha\beta} h_{\alpha\beta}(i) c_{\alpha}^*(\Omega_i) c_{\beta}(\Omega_i) = \sum_{\gamma} \Lambda_{\gamma}(i) |d_{\gamma}(\Omega_i)\rangle^2, \quad (10)$$

where the diagonalization is performed in the rightmost side by the unitary matrix  $V$ :  $d_{\gamma} = \sum_{\alpha} V_{\gamma\alpha}^{\dagger} c_{\alpha}$ . It is apparent at this point that the energy does not change by the phase transformation  $d_{\gamma} \rightarrow d_{\gamma} e^{i\theta_{\gamma}}$  for any  $\theta_{\gamma}$ , with which the coherent state is transformed as  $\Omega_i \rightarrow \Omega'_i$ . The parameter  $\theta_{\gamma}$  is determined to minimize the norm of the inner product  $\langle \Omega_i | \Omega'_i \rangle$  (see Ref. [68] for more details). This update makes it efficient to sample different configurations. We note that the above procedure involving coherent state reproduces the overrelaxation update usually used for the SU(2) case.

We show the numerical result of the classical Monte Carlo in Fig. 4. The calculation is performed for a finite-sized

lattice with  $N_{\text{site}} = 108 (= 4 \times 3^3)$  atoms where the lattice is created using primitive translation vectors. The temperature dependence of the specific heat is shown in Fig. 4(a) for the SU(2,4,6) models. At low temperatures, the specific heat takes  $2(N-1) \times \frac{1}{2}$  for the SU( $N$ ) model, which satisfies the equipartition theorem. Compared to the corresponding results of the mean-field calculation in Fig. 3(d), every model has the suppressed transition temperatures down to  $T_c \sim 10^{-3}$  eV because of the incorporation of spatial fluctuations. Figure 4(b) shows the  $\mathbf{q} = \mathbf{0}$  component of the static susceptibilities for the SU(6) model. For  $T \lesssim 10^{-3}$  eV, each component of the magnetic moments takes the huge values, showing the feature of second-order phase transition. The electric ( $Q$ ,  $G$ ) susceptibilities are characteristic for the SU(6) model and are absent in the SU(2) model.

*Classical equation of motion.* Using the path-integral approach, our framework can further address the thermodynamic nonequilibrium state. The equation of motion itself has already been derived by Zhang-Batista [55]. Their derivation is based on the Heisenberg equation of motion of  $\mathcal{O}_i^\xi$ , which gives  $N^2 - 1$  equations. In terms of the parameters of the coherent states, on the other hand, we only need  $2(N-1)$  equations. Hence some of those equations should be redundant.

Here, taking a different approach, we derive the least  $2(N-1)$  equations based on the principle of least action in Eq. (9) [82,88]. The resultant equation of motion for the local variable is given by

$$\sum_q \mathcal{B}_{pq}(i) \frac{\partial \Omega_{qi}}{\partial \tau} = - \frac{\partial \mathcal{H}}{\partial \Omega_{pi}}, \quad (11)$$

where  $\mathcal{H} = \langle \Omega | \mathcal{H}_{\text{eff}} | \Omega \rangle$  and the Berry curvature matrix is defined by

$$\mathcal{B}_{pq}(i) = \sum_\alpha \left( \frac{\partial c_\alpha^*(\Omega_i)}{\partial \Omega_{pi}} \frac{\partial c_\alpha(\Omega_i)}{\partial \Omega_{qi}} - \frac{\partial c_\alpha^*(\Omega_i)}{\partial \Omega_{qi}} \frac{\partial c_\alpha(\Omega_i)}{\partial \Omega_{pi}} \right), \quad (12)$$

with  $p, q = 1, \dots, 2(N-1)$ . Changing the time variable as  $\tau \rightarrow it$ , we obtain the real-time equation of motion. Since the analytic form of the Berry curvature matrix is obtained once the specific coherent state is given in Eq. (8), the even-dimension antisymmetric matrix  $\mathcal{B}$  in Eq. (11) is easily inverted numerically. Thus the explicit equation of motion is obtained for the  $2(N-1)$  classical variables, and will be used for a nonequilibrium dynamics in a realistic setup. The relation to the equations in Ref. [55] is not apparent but can

be deduced from the equation

$$- \frac{\partial \mathcal{O}_i^\xi}{\partial \tau} = \sum_{pq} \mathcal{B}_{pq}^{-1}(i) \frac{\partial \mathcal{O}_i^\xi}{\partial \Omega_{pi}} \frac{\partial \mathcal{H}}{\partial \Omega_{qi}}, \quad (13)$$

which derives from Eq. (11). The right-hand side is reminiscent of the commutator  $[\mathcal{O}_i^\xi, \mathcal{H}_{\text{eff}}]$ . The above equation of motion employing the SU( $N$ ) coherent state allows us to analyze not only the effect of space-time fluctuations on the ordered state, but also transport phenomena. The excitation spectra calculated from the obtained real-time equation of motion are expected to be the same as those from the flavor wave theory [56].

*Summary and outlook.* We have proposed the numerical calculation method for generic spin-orbital Mott insulators with  $N$  localized states, using SU( $N$ ) generators. Material-based analyses of spin-orbital Mott insulators with effective SU(2) models are limited to magnetic degrees of freedom. In contrast, our SU( $N$ ) formalism allows us to consider the electric degrees of freedom. Moreover, our framework can address many-body quantities such as double occupancy, which are not considered in conventional spin-orbital models.

We have applied this framework to 5d-pyrochlore oxides as a demonstration. The results from mean-field theory and classical Monte Carlo show the AIAO-type ordering with various spin-orbital order parameters and corresponding spin-orbital excitations, which substantiate the effectiveness of our approach. Our framework enables comprehensive analysis of various physical phenomena for materials with small quantum fluctuations. Although experimental results on Mott insulators in 5d-pyrochlore oxides with  $n=1$  are absent at present, application of our method to existing Mott insulators will provide useful insights by directly comparing the results with experiments.

We note that we cannot analyze exotic quantum states such as quantum liquids using the mean-field or the classical solvers. To address nonlocal quantum effects, quantum solvers, such as exact diagonalization or quantum Monte Carlo methods, are needed. A composite approach that integrates quantum, mean-field, and classical solvers will lead to a quantitative and systematic analysis of realistic spin-orbital Mott insulators such as iridates, trihalides, or organic compounds where strong quantum fluctuations exist. A detailed comparison between simulation results and experiments will provide us a deeper understanding of the Mott insulators, which leads to a design of functional materials.

*Acknowledgments.* The authors thank R. Pohle for fruitful discussions. H.S. thanks Y. Nomura for his help in constructing Wannier functions. This work was supported by KAKENHI Grants No. JP19H01842, No. JP21K03459, and No. JP22J10620.

- [1] A. Jain, Y. Shin, and K. A. Persson, *Nat. Rev. Mater.* **1**, 15004 (2016).
- [2] M. Imada, A. Fujimori, and Y. Tokura, *Rev. Mod. Phys.* **70**, 1039 (1998).
- [3] Y. Tokura and N. Nagaosa, *Science* **288**, 462 (2000).

- [4] B. J. Kim, H. Jin, S. J. Moon, J.-Y. Kim, B.-G. Park, C. S. Leem, J. Yu, T. W. Noh, C. Kim, S.-J. Oh, J.-H. Park, V. Durairaj, G. Cao, and E. Rotenberg, *Phys. Rev. Lett.* **101**, 076402 (2008).
- [5] G. Jackeli and G. Khaliullin, *Phys. Rev. Lett.* **102**, 017205 (2009).

- [6] B. J. Kim, H. Ohsumi, T. Komesu, S. Sakai, T. Morita, H. Takagi, and T. Arima, *Science* **323**, 1329 (2009).
- [7] W. Witczak-Krempa, G. Chen, Y. B. Kim, and L. Balents, *Annu. Rev. Condens. Matter Phys.* **5**, 57 (2014).
- [8] K. Kitagawa, T. Takayama, Y. Matsumoto, A. Kato, R. Takano, Y. Kishimoto, S. Bette, R. Dinnebier, G. Jackeli, and H. Takagi, *Nature (London)* **554**, 341 (2018).
- [9] Y. Kasahara, T. Ohnishi, Y. Mizukami, O. Tanaka, S. Ma, K. Sugii, N. Kurita, H. Tanaka, J. Nasu, Y. Motome, T. Shibauchi, and Y. Matsuda, *Nature (London)* **559**, 227 (2018).
- [10] N. Tang, Y. Gritsenko, K. Kimura, S. Bhattacharjee, A. Sakai, M. Fu, H. Takeda, H. Man, K. Sugawara, Y. Matsumoto, Y. Shimura, J. Wen, C. Broholm, H. Sawa, M. Takigawa, T. Sakakibara, S. Zherlitsyn, J. Wosnitzer, R. Moessner, and S. Nakatsuji, *Nat. Phys.* **19**, 92 (2023).
- [11] K. I. Kugel and D. I. Khomskii, *Pis'ma Zh. Eksp. Teor. Fiz.* **15**, 629 (1972) [*Sov. Phys. JETP Lett.* **15**, 446 (1972)].
- [12] K. I. Kugel and D. I. Khomskii, *Zh. Eksp. Teor. Fiz.* **64**, 1429 (1973) [*Sov. Phys. JETP* **37**, 725 (1973)].
- [13] M. Cyrot and C. Lyon-Caen, *Le J. de Phys.* **36**, 253 (1975).
- [14] G. Khaliullin and V. Oudovenko, *Phys. Rev. B* **56**, R14243(R) (1997).
- [15] S. Ishihara, J. Inoue, and S. Maekawa, *Phys. Rev. B* **55**, 8280 (1997).
- [16] L. F. Feiner and A. M. Oleś, *Phys. Rev. B* **59**, 3295 (1999).
- [17] S. Ishihara and S. Maekawa, *Phys. Rev. B* **62**, 2338 (2000).
- [18] A. B. Harris, A. Aharony, O. Entin-Wohlman, I. Y. Korenblit, and T. Yildirim, *Phys. Rev. B* **69**, 094409 (2004).
- [19] S. Ishihara, *Phys. Rev. B* **69**, 075118 (2004).
- [20] B. Normand and A. M. Oleś, *Phys. Rev. B* **78**, 094427 (2008).
- [21] J. Nasu and S. Ishihara, *Phys. Rev. B* **88**, 205110 (2013).
- [22] A. Koga, S. Nakauchi, and J. Nasu, *Phys. Rev. B* **97**, 094427 (2018).
- [23] J. Otsuki, K. Yoshimi, H. Shinaoka, and Y. Nomura, *Phys. Rev. B* **99**, 165134 (2019).
- [24] K. Bieniasz, M. Berciu, and A. M. Oleś, *Phys. Rev. B* **100**, 125109 (2019).
- [25] J. Nasu and M. Naka, *Phys. Rev. B* **103**, L121104 (2021).
- [26] G. Khaliullin, D. Churchill, P. P. Stavropoulos, and H.-Y. Kee, *Phys. Rev. Res.* **3**, 033163 (2021).
- [27] D. I. Khomskii, *ECS J. Solid State Sci. Technol.* **11**, 054004 (2022).
- [28] G. Zhang, E. Gorelov, E. Koch, and E. Pavarini, *Phys. Rev. B* **86**, 184413 (2012).
- [29] A. Chiesa, S. Carretta, P. Santini, G. Amoretti, and E. Pavarini, *Phys. Rev. Lett.* **110**, 157204 (2013).
- [30] Y. Yamaji, Y. Nomura, M. Kurita, R. Arita, and M. Imada, *Phys. Rev. Lett.* **113**, 107201 (2014).
- [31] J. G. Rau, E. K.-H. Lee, and H.-Y. Kee, *Phys. Rev. Lett.* **112**, 077204 (2014).
- [32] S. M. Winter, Y. Li, H. O. Jeschke, and R. Valentí, *Phys. Rev. B* **93**, 214431 (2016).
- [33] S. M. Winter, K. Riedl, and R. Valentí, *Phys. Rev. B* **95**, 060404(R) (2017).
- [34] D. Kurzydłowski and W. Grochala, *Phys. Rev. B* **96**, 155140 (2017).
- [35] A. Chiesa, E. Macaluso, P. Santini, S. Carretta, and E. Pavarini, *Phys. Rev. B* **99**, 235145 (2019).
- [36] Z. Huang, D. Liu, A. Mansikkamäki, V. Vieru, N. Iwahara, and L. F. Chibotaru, *Phys. Rev. Res.* **2**, 033430 (2020).
- [37] D. A. S. Kaib, S. Biswas, K. Riedl, S. M. Winter, and R. Valentí, *Phys. Rev. B* **103**, L140402 (2021).
- [38] D. Churchill and H.-Y. Kee, *Phys. Rev. B* **105**, 014438 (2022).
- [39] D. Fiore Mosca, L. V. Pourovskii, and C. Franchini, *Phys. Rev. B* **106**, 035127 (2022).
- [40] E. Pavarini, E. Koch, and A. I. Lichtenstein, *Phys. Rev. Lett.* **101**, 266405 (2008).
- [41] E. Pavarini and E. Koch, *Phys. Rev. Lett.* **104**, 086402 (2010).
- [42] C. Autieri, E. Koch, and E. Pavarini, *Phys. Rev. B* **89**, 155109 (2014).
- [43] M. Snamina and A. M. Oleś, *Phys. Rev. B* **94**, 214426 (2016).
- [44] J. Jeanneau, P. Toulemonde, G. Remenyi, A. Sulpice, C. Colin, V. Nassif, E. Suard, E. Salas Colera, G. R. Castro, F. Gay, C. Urdaniz, R. Weht, C. Fevrier, A. Ralko, C. Lacroix, A. A. Aligia, and M. Núñez-Regueiro, *Phys. Rev. Lett.* **118**, 207207 (2017).
- [45] A. A. Aligia and C. Helman, *Phys. Rev. B* **99**, 195150 (2019).
- [46] X.-J. Zhang, E. Koch, and E. Pavarini, *Phys. Rev. B* **105**, 115104 (2022).
- [47] L. V. Pourovskii, D. F. Mosca, and C. Franchini, *Phys. Rev. Lett.* **127**, 237201 (2021).
- [48] D. Fiore Mosca, L. V. Pourovskii, B. H. Kim, P. Liu, S. Sanna, F. Boscherini, S. Khmelevskiy, and C. Franchini, *Phys. Rev. B* **103**, 104401 (2021).
- [49] L. V. Pourovskii, *Phys. Rev. B* **108**, 054436 (2023).
- [50] A. M. Perelomov, *Commun. Math. Phys.* **26**, 222 (1972).
- [51] S. Gnutzmann and M. Kus, *J. Phys. A: Math. Gen.* **31**, 9871 (1998).
- [52] K. Nemoto, *J. Phys. A: Math. Gen.* **33**, 3493 (2000).
- [53] N. Read and S. Sachdev, *Nucl. Phys. B* **316**, 609 (1989).
- [54] E. M. Stoudenmire, S. Trebst, and L. Balents, *Phys. Rev. B* **79**, 214436 (2009).
- [55] H. Zhang and C. D. Batista, *Phys. Rev. B* **104**, 104409 (2021).
- [56] K. Remund, R. Pohle, Y. Akagi, J. Romhányi, and N. Shannon, *Phys. Rev. Res.* **4**, 033106 (2022).
- [57] D. Dahlbom, H. Zhang, C. Miles, X. Bai, C. D. Batista, and K. Barros, *Phys. Rev. B* **106**, 054423 (2022).
- [58] U. F. P. Seifert and L. Savary, *Phys. Rev. B* **106**, 195147 (2022).
- [59] D. Dahlbom, C. Miles, H. Zhang, C. D. Batista, and K. Barros, *Phys. Rev. B* **106**, 235154 (2022).
- [60] H. Zhang, Z. Wang, D. Dahlbom, K. Barros, and C. D. Batista, *Nat. Commun.* **14**, 3626 (2023).
- [61] S.-H. Do, H. Zhang, D. A. Dahlbom, T. J. Williams, V. O. Garlea, T. Hong, T.-H. Jang, S.-W. Cheong, J.-H. Park, K. Barros, C. D. Batista, and A. D. Christianson, *npj Quantum Mater.* **8**, 5 (2023).
- [62] R. Pohle, N. Shannon, and Y. Motome, *Phys. Rev. B* **107**, L140403 (2023).
- [63] J. S. Gardner, M. J. P. Gingras, and J. E. Greedan, *Rev. Mod. Phys.* **82**, 53 (2010).
- [64] H. Shinaoka, Y. Motome, T. Miyake, S. Ishibashi, and P. Werner, *J. Phys.: Condens. Matter* **31**, 323001 (2019).
- [65] H. Shinaoka, T. Miyake, and S. Ishibashi, *Phys. Rev. Lett.* **108**, 247204 (2012).
- [66] J. Yamaura, K. Ohgushi, H. Ohsumi, T. Hasegawa, I. Yamauchi, K. Sugimoto, S. Takeshita, A. Tokuda, M. Takata, M. Udagawa, M. Takigawa, H. Harima, T. Arima, and Z. Hiroi, *Phys. Rev. Lett.* **108**, 247205 (2012).
- [67] G. Kotliar, S. Y. Savrasov, K. Haule, V. S. Oudovenko, O. Parcollet, and C. A. Marianetti, *Rev. Mod. Phys.* **78**, 865 (2006).

- [68] See Supplemental Material at <http://link.aps.org/supplemental/10.1103/PhysRevB.108.L241108> for details on the first-principles calculations, the derivation of the effective Hamiltonian, the construction of  $SU(N)$  generators, definitions of the physical quantities, the  $SU(N)$  coherent state, the overrelaxation update in the classical Monte Carlo calculation, and the application to the simplest  $N = 2$  case. The Supplemental Material includes Refs. [89–96].
- [69] D. J. Singh, P. Blaha, K. Schwarz, and J. O. Sofo, *Phys. Rev. B* **65**, 155109 (2002).
- [70] H. Harima, *J. Phys. Chem. Solids* **63**, 1035 (2002).
- [71] H. Shinaoka, S. Hoshino, M. Troyer, and P. Werner, *Phys. Rev. Lett.* **115**, 156401 (2015).
- [72] K. Momma and F. Izumi, *J. Appl. Cryst.* **44**, 1272 (2011).
- [73] S. Ôkubo, *Prog. Theor. Phys.* **12**, 603 (1954).
- [74] C. Bloch, *Nucl. Phys.* **6**, 329 (1958).
- [75] J. des Cloizeaux, *Nucl. Phys.* **20**, 321 (1960).
- [76] P. Durand, *Phys. Rev. A* **28**, 3184 (1983).
- [77] Y. Kuramoto, *Quantum Many-Body Physics*, Vol. 934 (Springer, Japan, 2020).
- [78] R. Iwazaki and S. Hoshino, *Phys. Rev. B* **103**, 235145 (2021).
- [79] K. Tomiyasu, K. Matsuhira, K. Iwasa, M. Watahiki, S. Takagi, M. Wakeshima, Y. Hinatsu, M. Yokoyama, K. Ohoyama, and K. Yamada, *J. Phys. Soc. Jpn.* **81**, 034709 (2012).
- [80] H. Sagayama, D. Uematsu, T. Arima, K. Sugimoto, J. J. Ishikawa, E. O'Farrell, and S. Nakatsuji, *Phys. Rev. B* **87**, 100403(R) (2013).
- [81] S. M. Disseler, *Phys. Rev. B* **89**, 140413(R) (2014).
- [82] A. Auerbach, *Interacting Electrons and Quantum Magnetism* (Springer, New York, 1994).
- [83] E. H. Lieb, *Commun. Math. Phys.* **31**, 327 (1973).
- [84] K. Hukushima and K. Nemoto, *J. Phys. Soc. Jpn.* **65**, 1604 (1996).
- [85] M. Creutz, *Phys. Rev. D* **36**, 515 (1987).
- [86] D. Landau and K. Binder, *A Guide to Monte Carlo Simulations in Statistical Physics* (Cambridge University Press, Cambridge, 2021).
- [87] J. L. Alonso, A. Tarancón, H. G. Ballesteros, L. A. Fernández, V. Martín-Mayor, and A. M. Sudupe, *Phys. Rev. B* **53**, 2537 (1996).
- [88] N. Nagaosa, *Quantum Field Theory in Condensed Matter Physics* (Springer, Berlin, 1999).
- [89] P. Giannozzi, S. Baroni, N. Bonini, M. Calandra, R. Car, C. Cavazzoni, D. Ceresoli, G. L. Chiarotti, M. Cococcioni, I. Dabo, A. D. Corso, S. de Gironcoli, S. Fabris, G. Fratesi, R. Gebauer, U. Gerstmann, C. Gougoussis, A. Kokalj, M. Lazzeri, L. Martin-Samos *et al.*, *J. Phys.: Condens. Matter* **21**, 395502 (2009).
- [90] P. Giannozzi, O. Andreussi, T. Brumme, O. Bunau, M. B. Nardelli, M. Calandra, R. Car, C. Cavazzoni, D. Ceresoli, M. Cococcioni, N. Colonna, I. Carnimeo, A. D. Corso, S. de Gironcoli, P. Delugas, R. A. DiStasio, A. Ferretti, A. Floris, G. Fratesi, G. Fugallo *et al.*, *J. Phys.: Condens. Matter* **29**, 465901 (2017).
- [91] A. A. Mostofi, J. R. Yates, G. Pizzi, Y.-S. Lee, I. Souza, D. Vanderbilt, and N. Marzari, *Comput. Phys. Commun.* **185**, 2309 (2014).
- [92] A. Dal Corso, *Comput. Mater. Sci.* **95**, 337 (2014).
- [93] P. E. Blöchl, *Phys. Rev. B* **50**, 17953 (1994).
- [94] D. Mandrus, J. R. Thompson, R. Gaal, L. Forro, J. C. Bryan, B. C. Chakoumakos, L. M. Woods, B. C. Sales, R. S. Fishman, and V. Keppens, *Phys. Rev. B* **63**, 195104 (2001).
- [95] D. J. Klein, *J. Chem. Phys.* **61**, 786 (1974).
- [96] H. Georgi, *Lie Algebras in Particle Physics*, 2nd ed. (Perseus Books, New York, 2000).